Geophys. J. Int. (1999) **138,** 563–570

Frequency–magnitude statistics and spatial correlation dimensions of earthquakes at Long Valley caldera, California

D. J. Barton,[1] G. R. Foulger,[1] J. R. Henderson[1,*] and B. R. Julian[2]

[1] *Department of Geological Sciences, University of Durham, Durham,* DH1 3LE, *UK. E-mail: g.r.foulger@durham.ac.uk*
[2] *US Geological Survey, Menlo Park,* CA 94025, *USA*

Accepted 1999 April 6. Received 1999 March 17; in original form 1998 June 2

SUMMARY

Intense earthquake swarms at Long Valley caldera in late 1997 and early 1998 occurred on two contrasting structures. The first is defined by the intersection of a north-northwesterly array of faults with the southern margin of the resurgent dome, and is a zone of hydrothermal upwelling. Seismic activity there was characterized by high *b*-values and relatively low values of *D*, the spatial fractal dimension of hypocentres. The second structure is the pre-existing South Moat fault, which has generated large-magnitude seismic activity in the past. Seismicity on this structure was characterized by low *b*-values and relatively high *D*. These observations are consistent with low-magnitude, clustered earthquakes on the first structure, and higher-magnitude, diffuse earthquakes on the second structure. The first structure is probably an immature fault zone, fractured on a small scale and lacking a well-developed fault plane. The second zone represents a mature fault with an extensive, coherent fault plane.

Key words: earthquakes, fractal, Long Valley.

1 INTRODUCTION

The seismic *b*-value of a set of earthquakes is the negative slope of the log-cumulative-frequency versus magnitude plot. It is a measure of the proportion of larger to smaller events within a seismic sequence. A low value of *b* indicates a greater proportion of larger events than in the case where the value of *b* is high. The spatial correlation dimension of hypocentres, *D*, is a measure of the scaling in the spatial distribution of events. Correlations between *b* and *D*, both positive and negative, have been reported both in natural earthquake data (e.g. Hirata 1989; Henderson *et al.* 1994) and in laboratory tests (e.g. Meredith *et al.* 1990). Physical models have been proposed to explain these correlations (e.g. Henderson & Main 1992) but the causative physical processes are still under debate.

In this study, the *b*-value and the spatial correlation dimension are calculated for recent volcanic earthquakes from the Long Valley caldera, California, recorded on the permanent Northern California Seismic Network (NCSN). The seismic *b*-value, *D* and the correlation between them change significantly as the locus of seismicity changes over time. These changes correspond to an abrupt change in the nature of local crustal deformation and the transition from volcanic swarm-type seismicity to seismic activation of the pre-existing South Moat fault near the southern caldera rim.

* Currently at: Elf Exploration UK PLC, Aberdeen.

2 TECTONIC SETTING AND DATA

Long Valley caldera lies on the eastern side of the Sierra Nevada in east-central California (Fig. 1). The caldera formed at about 0.76 Ma when a magmatic system erupted cataclysmically and emplaced 600 km^3 of material (Bailey *et al.* 1976). A ring fault formed, on which 2–3 km of subsidence occurred, forming a 17×32 km oval depression. Subsequent magmatic activity in the centre of the caldera built a resurgent dome.

The current period of unrest in Long Valley commenced in 1978 with an $M = 5.7$ earthquake 20 km south of the caldera (Rundle & Hill 1988). In 1980, there was a seismic crisis with four $M \sim 6$ earthquakes. Since then, seismic activity has been almost continuous with occasional events as large as $M = 5.5$. The Mammoth Mountain area at the southwestern edge of the caldera vents 400–500 tonnes of CO_2 per day (Farrar *et al.* 1995). Uplift of the resurgent dome also commenced in 1980 and continues to the present day. The deformation pattern is consistent with the inflation of an underlying magma chamber at depths of 6–10 km (Rundle & Hill 1988).

Since June 1997 there has been a great increase in seismic activity to the immediate south of the resurgent dome, culminating in a massive swarm of >2000 earthquakes during the period 1997 November 22–25. This increase in seismicity coincided with accelerated inflation of the resurgent dome. Ground deformation was monitored by two-colour geodimeter, GPS, tiltmeter and strainmeter measurements.

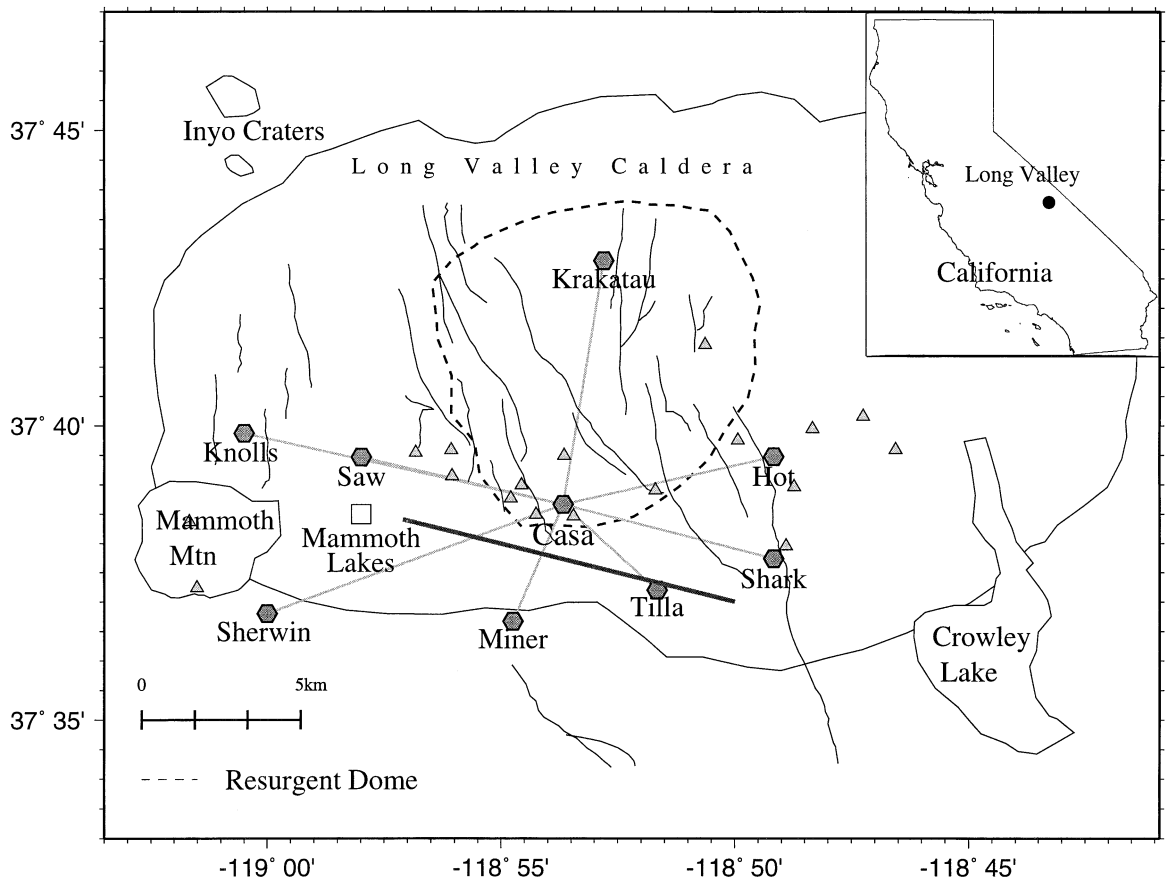

Figure 1. Map of Long Valley caldera showing regional location (inset) and main tectonic features. The caldera rim is indicated by a solid line, and the resurgent dome by a dashed line. Thin lines: faults; triangles: hot springs and fumaroles; solid grey line: the South Moat fault. The two-colour Geodimeter stations are shown (hexagons), and grey lines joining them indicate baselines routinely measured. The town of Mammoth Lakes is indicated by a square. Map features from Sorey (1985).

Earthquakes at Long Valley are continually monitored by the NCSN network, which has approximately 50 stations within 50 km of the caldera. The NCSN catalogue contains both earthquake locations and magnitudes based on measurements made by hand (CUSP data) and automatically picked measurements (Earthworm data). The CUSP and Earthworm results are merged in the catalogue, with the CUSP results taking precedence where both exist. Between 1997 January and 1998 February, 24 511 earthquakes were catalogued, 4820 of which were CUSP-processed. The majority occurred in swarms between 1997 July and November.

During periods of relatively low activity, CUSP-processed events are complete down to $M = 1.2$. During intense swarms, however, staff time is only sufficient to hand pick the largest events and many earthquakes larger than $M = 1.2$ are processed only by the Earthworm system. In addition to having less accurate locations, Earthworm magnitudes are determined from coda lengths, and several closely spaced events may be interpreted as a single large event. This causes exaggeration of the numbers of large-magnitude events and underestimation of the numbers of low-magnitude events. The effect of this during intense swarms can be seen from log-cumulative-frequency versus magnitude plots (Fig. 2). During periods of low activity (Fig. 2a), a straight-line distribution following the Gutenberg–Richter equation is exhibited for earthquakes with $M \geq 1.2$. During intense swarms (Fig. 2b), however, a distorted log-cumulative-frequency versus magnitude plot results, which may exhibit two straight segments above $M = 1.2$, and a correct b-value cannot be calculated. We therefore restrict our analyses to those time periods where CUSP data are complete down to a threshold value of $M = 1.8$. By using only the CUSP data we increase our confidence that the observed differences in b-value are real, and do not arise from systematic errors in automatic magnitude calculation. Furthermore, this restricts our data set to the most accurately located earthquakes.

3 METHOD

The threshold magnitude was selected by examining plots of log-cumulative-frequency versus magnitude. A threshold magnitude of $M = 1.8$ was the lowest suitable for the data set used in this study. We used sliding windows of 200 data points to estimate both b and D, with each window overlapping the next by 10 events (Fig. 3).

The hypocentral spatial distribution of the CUSP events for 200-event windows was characterized by the correlation dimension D (Grassberger & Procaccia 1983):

$$D = \lim_{r \to 0} \frac{\log C(r)}{\log r},$$

where r is the radius of the sphere of investigation, and $C(r)$, the correlation integral, is a measure of the fraction of pairs of

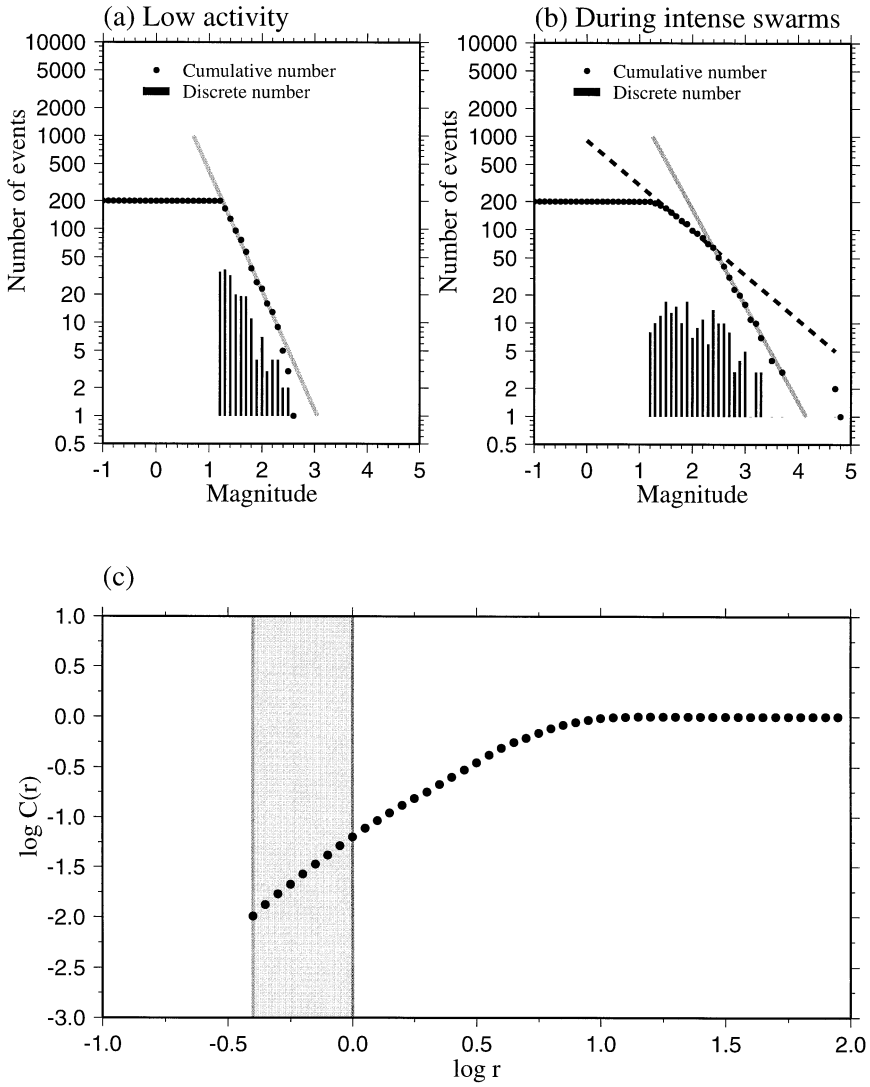

Figure 2. Examples of b and D calculated using samples of all the data (CUSP and Earthworm) from the NCSN catalogue. (a) Plot of log-cumulative-frequency versus magnitude for data from June 1997 when the CUSP (hand-picked) magnitude threshold was $M = 1.2$. There is a linear relationship above $M = 1.2$. (b) As (a), but for data from late November 1997 during an intense swarm. A highly non-linear plot for earthquakes larger than $M = 1.2$ results, and the threshold indicated on the plot is $M = 2.4$. (c) A typical plot of $\log C(r)$ versus $\log r$ showing the range selected for calculating D (shaded area).

earthquakes having separations $< r$. In the case of an infinite fractal distribution, a plot of $\log C(r)$ against $\log r$ will be a straight line whose gradient is the fractal dimension. A finite data sample typically yields a plot that is only linear for that range of r that is above the depopulation limit and below the saturation limit. In this study we estimate the fractal dimension for values of r of $0.4 < r < 1$ km (Fig. 2c).

Although previous work has suggested that large data sets are required to calculate D accurately (Smith 1988), there is evidence that much smaller data sets are adequate, particularly in situations where it is differences in fractal dimension that are of interest rather than their absolute values (Nerenberg & Essex 1990). This conclusion is supported by the findings of Havstad & Ehlers (1989) and Eneva (1996).

The value of D is an indicator of clustering within the earthquake population. Earthquakes that are diffuse in space are characterized a large value of D. As the earthquakes become progressively more clustered the value of D decreases.

The range of magnitudes is small. For this reason we estimate the b-value using the maximum likelihood method of Page (1968)

4 RESULTS

Changes in the values of b and D are shown in Fig. 3, and the spatial distributions of the events in various time windows are shown in Figs 4–6. Prior to 1997 November 22, most of the earthquakes occurred in clusters which together formed a broad zone trending N85°E along the southern margin of the resurgent dome and to its immediate southwest (Fig. 4). During the period that seismicity occurred in this area, b was relatively high and D relatively low, consistent with low-magnitude, clustered activity (Fig. 3a). There is a negative correlation between b and D (Fig. 3b).

Commencing 1997 November 22 there is a sharp fall in b, accompanied by a sharp rise in D. The b-value had mostly

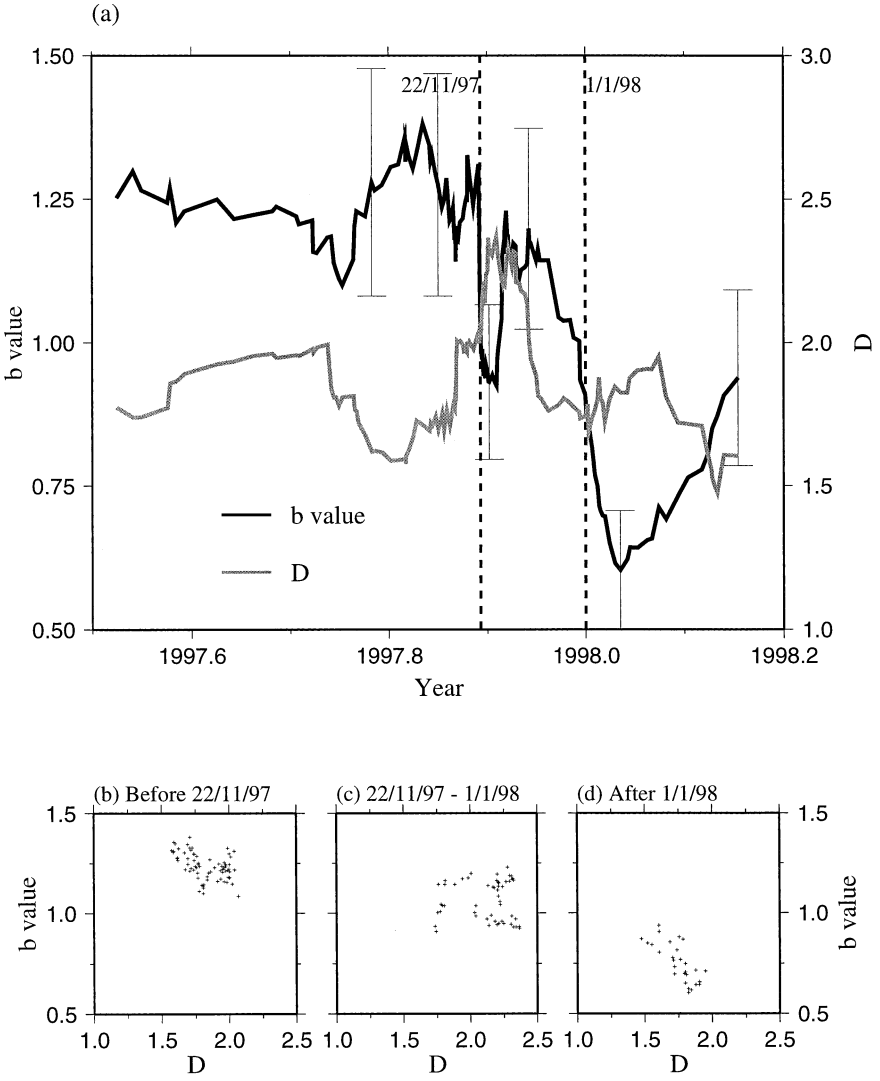

Figure 3. (a) Plot of *b* and *D* for 200-event windows for the period 1997 January 1 to 1998 February 28. Few CUSP-processed earthquakes were catalogued during the first half of 1997. The error bars for *b* correspond to the 95 per cent confidence limits. The errors in *D* are ~10 per cent of the calculated value (Henderson *et al.* 1992; Havstad & Ehlers 1989). (b) Plot of *b* versus *D* for the period 1997 January 1 to 1997 November 21; (c) as (b) but for the period 1997 November 22 to 1997 December 31; (d) as (b) but for the period 1998 January 1 to 1998 February 28.

recovered by 1997 December 5, from which date both *b* and *D* decreased overall until 1998 January 1. Between 1997 November 22 and 1998 January 1, *b* and *D* are uncorrelated (Fig. 3c). During this period the seismicity formed a much narrower, linear zone trending N105°E and located 2–3 km south of the pre-November 22 activity (Fig. 5). This linear feature dips at 80° and contains several events with $M > 4.0$. The relatively high values of *D* indicate that the activity is diffuse.

After 1998 January 1 there was again a negative correlation between *b* and *D* (Fig. 3d). There was also a return to a pattern of clusters further north, on the southern edge of the resurgent dome (Fig. 6).

5 DISCUSSION

Prior to November 22, clustered earthquake activity formed an easterly trending zone beneath the southern margin of the resurgent dome. This zone coincides with the distribution of thermal springs and fumaroles which occur where north-northwesterly trending faults cross the southern edge of the resurgent dome (Fig. 1). The seismic activity was probably caused by accelerated resurgent dome uplift, causing extension and allowing the migration of hot fluids up this zone (Foulger *et al.* 1998).

The linear seismic feature activated on and after November 22 coincides with the South Moat fault, a blind, subvertical, strike-slip fault (Denlinger *et al.* 1985). Motion on this fault may have been facilitated by the same processes that gave rise to the nearby pre-November 22 seismicity, or by processes resulting from that activity.

The change in locus of seismicity is associated with a change in locus of deformation as suggested by geodetic measurements. Prior to November 22, rapid dome inflation occurred, with the greatest line lengthening on the two-colour geodimeter lines Casa to Krakatau, Saw, Hot and Knolls (Fig. 1). Between November 22 and 26, accelerated lengthening occurred on the Casa–Krakatau and Casa-Saw lines, but lengthening ceased

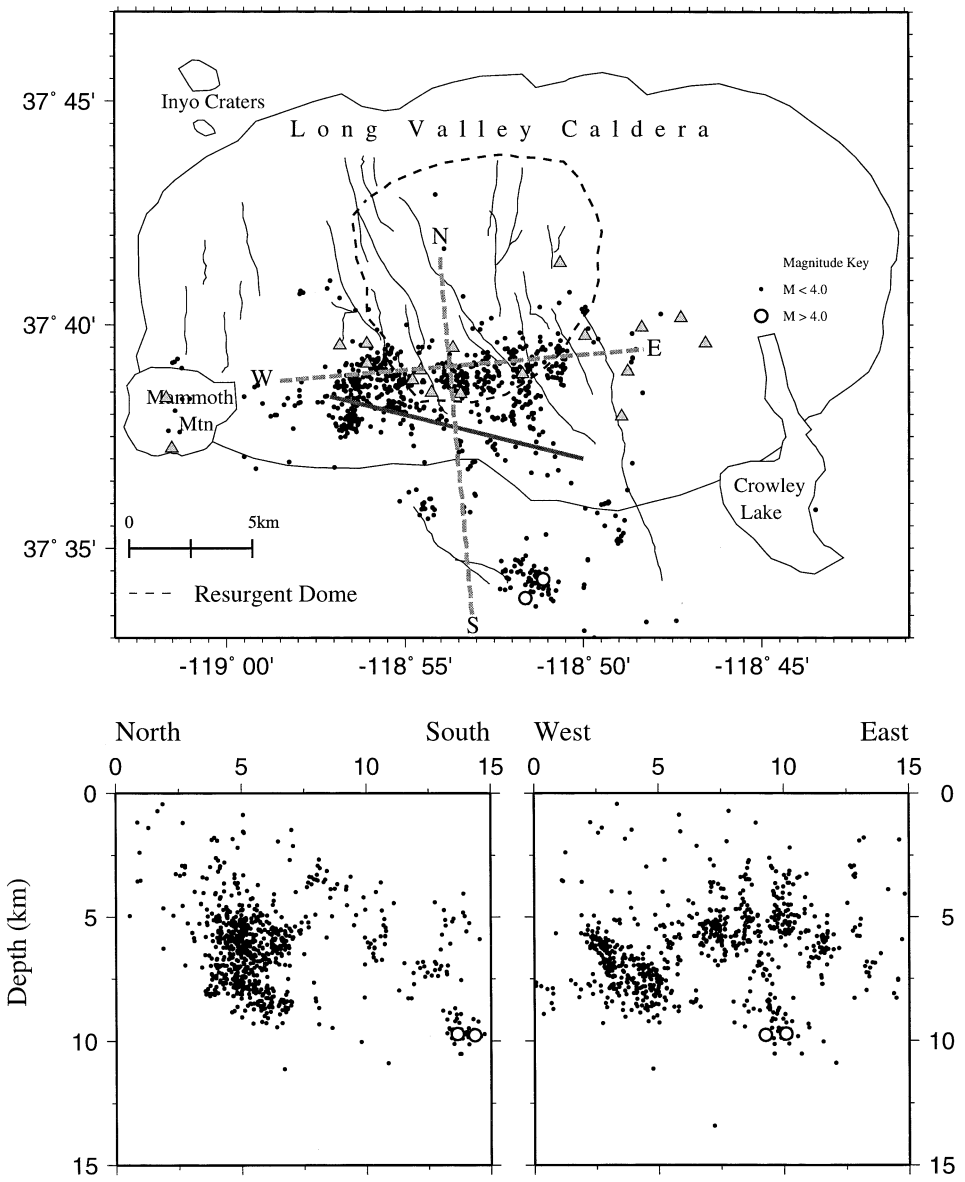

Figure 4. Seismicity in Long Valley for the period 1997 January 1 to 1997 November 21. Events with $M \geq 1.8$ are shown. Events with $M \geq 4$ are shown as open circles. Map features as for Fig. 1. (a) Earthquake epicentres; (b) north–south cross-section; (c) west–east cross-section. On the cross-sections, events within ± 10 km of the lines of section shown in (a) are plotted.

on the Casa–Hot and Casa–Knolls lines. The lines Casa–Tilla and Casa–Miner began to contract. After November 26 the rate of lengthening for the Casa–Krakatau line decreased, and the rates of lengthening of the Casa–Knolls, Casa–Saw and Casa–Sherwin lines increased abruptly. Also, the Casa–Tilla, Casa–Shark and Casa–Hot lines started to shorten. Detailed modelling of the data has yet to be done, but these observations suggest that the locus of greatest deformation moved from beneath the resurgent dome to an area between the geodimeter stations Casa, Miner, Tilla and Saw—the same area as the most intense seismicity on the narrow linear zone that was activated after November 22.

A number of reasons for variations in *b*-value have been suggested. Mogi (1962) pointed to the importance of heterogeneity in contributing to high *b*-value. Scholz (1968) demonstrated an inverse correlation between stress level and *b*-value in laboratory experiments. Stress level may be affected by pore fluid pressure and thermal stresses, and these have also been proposed as contributing to variations in *b*-value (Warren & Latham 1970; Wyss 1973). High stress levels at asperities suggest a means of mapping the latter using *b*-values (Wiemer & Wyss 1997). Furthermore, changes in stress levels and degrees of heterogeneity may lead to temporal variations in *b*-value (e.g. Wiemer & McNutt 1997). Wiemer *et al.* (1998) have presented a study of seismicity at Long Valley which demonstrates that changes in seismicity can be related to changes in the nature of magmatic activity. Examples of short- to intermediate-term temporal variation in *b*-value are also presented by Henderson & Main (1992) and Henderson *et al.* (1994). In addition, Henderson & Main (1992) suggest a mechanism by which *b*-values will change over time even in the absence of changes in the external stress, as a consequence

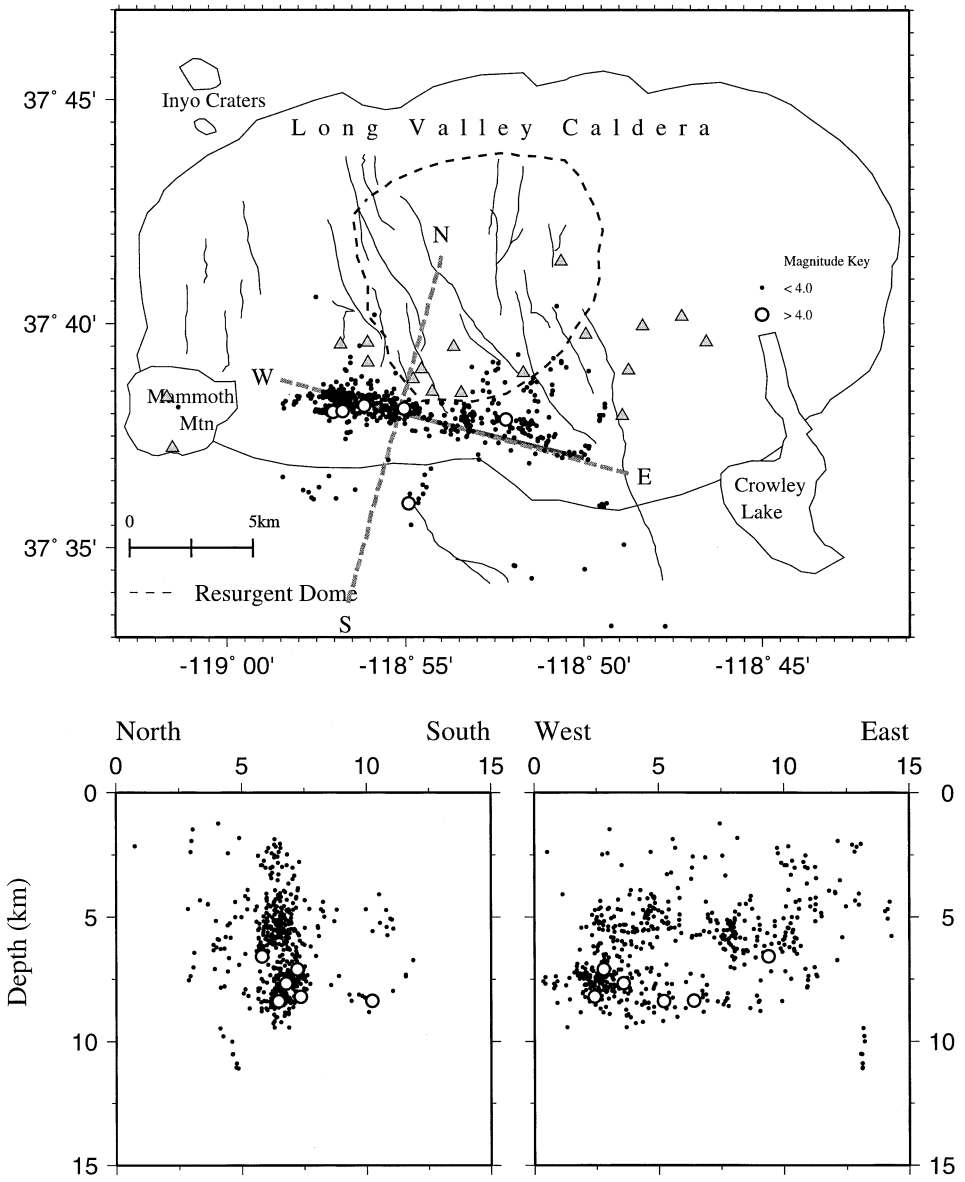

Figure 5. As Fig. 4, but for the period 1997 November 22 to 1997 December 31.

of non-linear feedback processes resulting in changes in stress intensity factor associated with the growing population of cracks.

In the examples described here we suggest that variations in b and D can be explained by considering the different processes operating in the various regimes. In the hydrothermal zone of weakness that was active prior to November 22, many small faults and small-scale structures, possibly augmented by thermal cracking, provided a highly heterogeneous environment. High permeability and a supply of pore fluids may have resulted in reduced effective stresses, and thus the earthquakes were caused by the failure of isolated, small asperities and consequently occurred in clusters. This resulted in high b and relatively low D. This is consistent with the weak negative correlation shown in Fig. 3(b).

From November 22, seismic activity was transferred to the South Moat fault. This fault has failed in the past with $M > 6$ earthquakes and has a mature, well-developed, coherent fault plane. Highly stressed asperities are widely spaced along it. Consequently, when it failed large-magnitude earthquakes occurred, causing a low b-value. The wide distribution of earthquakes along the fault plane caused a relatively high value of D.

This study describes an unusual case where adjacent structures with contrasting seismic properties are activated and monitored using a uniform network and data processing techniques, and sufficient earthquakes are available to yield many accurate estimates of b and D. It also shows that the South Moat fault is a subvertical blind fault $\sim$12 km long and $\sim$7 km high, terminating at its western end $\sim$1 km east of the town of Mammoth Lakes. Its history of $M > 6$ earthquakes and its behaviour during the 1997–1998 period of activation show that, in contrast to the hydrothermal zone a few kilometres further north, it is capable of generating large-magnitude earthquakes. It thus represents a potential hazard to the town of Mammoth Lakes.

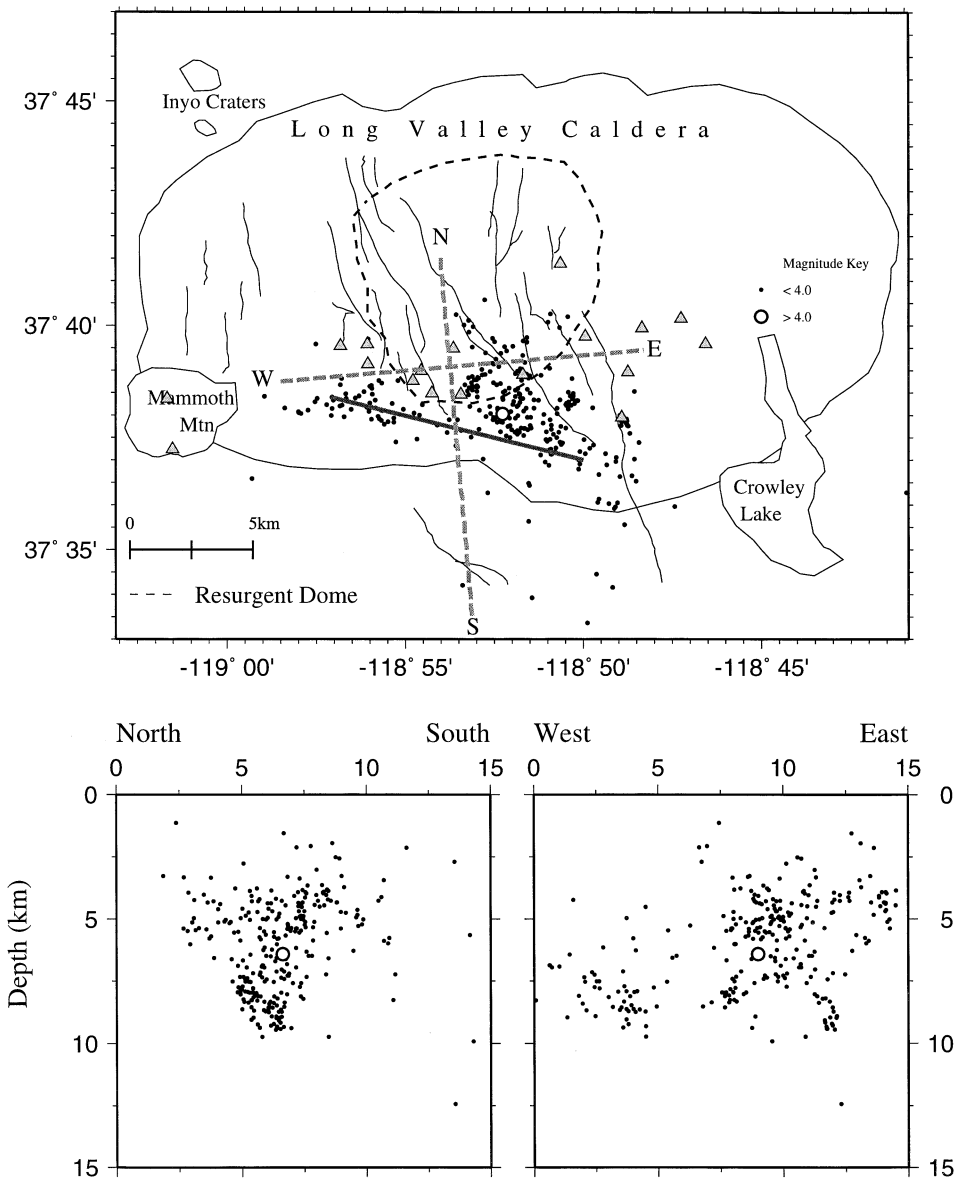

Figure 6. As Fig. 4, but for the period 1998 January 1 to 1998 February 28.

ACKNOWLEDGMENTS

The seismic data were obtained from the NCSN catalogue at Berkeley. Valuable advice was given by Mitch Pitt and David Oppenheimer, and the geodimeter data were kindly supplied by John Langbein, all at the USGS. DJB was supported by a NERC research studentship. We are grateful for the very thorough reviews of Max Wyss and an anonymous reviewer who pointed out a major error in the original manuscript.

REFERENCES

Bailey, R.A., Dalrymple, G.D. & Lanphere, M.A., 1976. Volcanism, structure and geochronology of Long Valley Caldera, Mono County, California, *J. geophys. Res.,* **81,** 725–744.

Denlinger, R.P., Riley, F.S., Boling, J.K. & Carpenter, M.C., 1985. Deformation of Long Valley Caldera between August 1982 and August 1983, *J. geophys. Res.,* **90,** 11 199–11 209.

Eneva, M., 1996. Effect of limited datasets in evaluating the scaling properties of spatially distributed data: an example from mining induced seismic activity, *Geophys. J. Int.,* **124,** 773–786.

Farrar, C.D., Sorey, M.L., Evans, W.C., Howle, J.F., Kerr, B.D., Kennedy, B.M., King, C.-Y. & Southon, J.R., 1995. Forest-killing diffuse CO_2 emission at Mammoth Mountain as a sign of magmatic unrest, *Nature,* **336,** 675–678.

Foulger, G.R., Malin, P.E., Shalev, E., Julian, B.R. & Hill, D.P., 1998. Seismic monitoring and activity increase in California caldera, *EOS, Trans. Am. geophys. Un.,* **79,** 357–363.

Grassberger, P. & Procaccia, I., 1983. Measuring the strangeness of strange attractors, *Physica,* **9D,** 189–208.

Havstad, J.W. & Ehlers, C.L., 1989. Attractor dimension of non-stationary dynamical systems from small data sets, *Phys. Rev.,* **39,** 845–853.

Henderson, J.R. & Main, I.G., 1992. A simple fracture-mechanical model for the evolution of seismicity, *Geophys. Res. Lett.,* **19,** 365–368.

Henderson, J.R., Main, I.G., Pearce, R.G. & Takeya, M., 1994. Seismicity in north-eastern Brazil: fractal clustering and the evolution of the B-value, *Geophys. J. Int.,* **116,** 217–226.

Hirata, T., 1989. A correlation between the B-value and fractal dimension of earthquakes, *J. geophys. Res.,* **94,** 7507–7514.

Meredith, P.G., Main, I.G. & Jones, C., 1990. Temporal variations in seismicity during quasi-static and dynamic rock failure, *Tectonophysics,* **175,** 249–268.

Mogi, K., 1962. Magnitude–frequency relation for elastic shocks accompanying fractures of various materials and some related problems in earthquakes, *Bull. Earthq. Res. Inst. Univ. Tokyo,* **40,** 831–853.

Nerenberg, M.A.H. & Essex, C., 1990. Correlation dimension and systematic geometric effects, *Phys. Rev.,* **42,** 7065–7074.

Page, R., 1968. Aftershocks and micro-aftershocks of the Great Alaska Earthquake of 1964, *Bull. seism. Soc. Am.,* **58,** 1131–1168.

Rundle, J.B. & Hill, D.P., 1988. The geophysics of a restless caldera—Long Valley, California, *Ann. Rev. Earth planet. Sci.,* **16,** 251–271.

Scholz, C.H., 1968. The frequency–magnitude relation of microfracturing in rock and its relation to earthquakes, *Bull. seism. Soc. Am.,* **58,** 399–415.

Smith, L.A., 1988. Intrinsic limits on dimension calculations, *Phys. Lett.,* **113,** 283–288.

Sorey, M.L., 1985. Evolution and present state of the hydrothermal system in Long Valley Caldera, *J. geophys. Res.,* **90,** 11 219–11 228.

Warren, N.W. & Latham, G.V., 1970. An experimental study of thermally induced microfracturing and its relation to volcanic seismicity, *J. geophys. Res.,* **75,** 4455–4464.

Wiemer, S. & McNutt, S., 1997. Variations in frequency–magnitude distribution with depth in two volcanic areas: Mount St. Helens, Washington, and Mt. Spurr, Alaska, *Geophys. Res. Lett.,* **24,** 189–192.

Wiemer, S. & Wyss, M., 1997. Mapping the frequency–magnitude distribution in asperities: an improved technique to calculate recurrence times, *J. geophys. Res.,* **102,** 15 115–15 128.

Wiemer, S., McNutt, S.R. & Wyss, M., 1998. Temporal and three-dimensional spatial analyses of the frequency–magnitude distribution near Long Valley caldera, California, *Geophys. J. Int.,* **134,** 409–421.

Wyss, M., 1973. Towards a physical understanding of the earthquake frequency distribution, *Geophys. J. R. astr. Soc.,* **31,** 341–359.